Critical Current Density and Current Transfer Length of Multifilamentary MgB_2 Strands of Various Design

G Z Li[1], K M Reddy[1], J B Zwayer[1], M A Kuldell[1], M A Susner[1], Y Yang[1], M D Sumption[1], J J Yue[2], M A Rindfleisch[2], M J Tomsic[2], C J Thong[2] and E W Collings[1]

***Abstract*—In this paper, a series of high performing *PIT* MgB_2 strands have been prepared. Transport voltage-current measurements were performed to determine the effects of C doping and strand geometry such as filament numbers. The best J_c for our samples was 1.0×10^5 A/cm^2 at 4.2 K, 7 T, for a strand using B powder with 3% C addition. The current transfer length (CTL) was also measured for MgB_2 short wires with Nb chemical barrier and Monel outer sheath. The CTL ranged from 2-12 mm, and had a correlation with the filament numbers.**

***Index Terms*—Magnesium diboride, critical current density, n-value, current transfer length.**

I. Introduction

TO OBTAIN an MgB_2 strand which is capable of finding its niche alongside other superconductors like NbTi or Nb_3Sn, it is necessary to enhance the critical current density J_c obtainable with applied magnetic field. Many methods, including chemical doping [2], [3], hot pressing [4], cold high pressure pressing [5], mechanical alloying [6] and Mg infiltration or diffusion [7]-[9], have been used to improve J_c, especially at high fields. Meanwhile, by adopting proper sheath materials [10], chemical barriers [11] and strand geometry [12], MgB_2 strands with useful J_cs can be achieved. We show in this paper some influence of C doping and strand design on J_c as well as n-value, which is important for device applications.

In addition to the study of J_c and n, it is useful to understand the length required for current transfer into the strand. All superconducting strands require a certain distance over which current injected into the wire from the outside transfers in to the superconducting filaments. There is a voltage profile associated with the penetration of current into the superconducting filaments from the outside resistive sheathes and barriers. The voltage at a given distance from the current injection region increases with applied current, and drops with distance away from this region, eventually reaching zero the voltage tap is sufficiently far away. This minimum distance is defined as current transfer length, or CTL. Ekin *et al.* studied the CTL of NbTi and Nb_3Sn, stating that the CTL of a superconductor is determined by the wire diameter, the resistivity of sheath materials and n-values [13]. Holubek *et al.* measured a monocore MgB_2/Fe wire and found its CTL to be below 10 mm in an applied field of 5.2 T with the conductor carrying 31.7 A [14]. In their subsequent investigation of MgB_2 wires with different sheaths (Fe, Nb/Fe, FeNiCo and Nb/AgMg) and wire geometries (1 or 4 filaments), they reported an applied-current-independent CTL parameter λ as 0.35-2 mm in typical conductors [15] by fitting sample surface potentials along wire length direction with an equation previously expressed by Wilson [16]. With this method, their previously reported monocore MgB_2/Fe wire had λ of about 0.6 mm.

In this work, we first examined three series of continuous-tube-filling-forming-type (*CTFF*) [17] powder-in-tube (*PIT*) long strands with different C doping levels and strand geometries. The effects of doping concentration and filament numbers were investigated. Secondly, the CTLs of *CTFF*-type *PIT* short wires with Nb/monel sheaths, either monocore or multifilamentary were measured.

II. Experimental

A. Samples

A series of MgB_2 strands were fabricated by Hyper Tech Research, Inc. using the continuous-tube-filling-forming route. All the samples used fine B powder (10-100 nm particle size) from Specialty Materials Inc. produced by the plasma assisted reaction of BCl_3 with H_2 and *in situ* C doped by adding CH_4 to the process gases [18]. After drawn to the designated wire diameter, these strands were heat treated in a tube furnace by ramping to soak temperature in about 80 min, then holding that temperature for a suitable time and then furnace cooling to room temperature. The soak temperature was chosen between 650 ºC and 700 ºC based on extensive experience that little variation in J_c was found with heat treatment temperature at 650 ºC to 700 ºC for suitable times. The strand specifications including C doping level, filament numbers, wire diameter, and heat treatment conditions are listed in Table I.

B. Characterizations

Transport voltage-current measurements were performed on all samples at 4.2 K in pool boiling liquid He in transverse

Manuscript received October 4, 2012. This work was supported by the U.S. Department of Energy, High Energy Physics grant DE-FG02-95ER40900, and a DOE SBIR.

G Z Li, K M Reddy, J B Zwayer, M A Kuldell, M A Susner, Y Yang, M D Sumption and E W Collings are with Center for Superconducting and Magnetic Materials, Department of Materials Science and Engineering, The Ohio State University, Columbus, OH, 43210 USA (e-mail: li.1423@osu.edu).

J J Yue, M A Rindfleisch, C J Thong and M J Tomsic are with Hyper Tech Research, Inc, Columbus, OH, 43228 USA.

TABLE I STRAND SPECIFICATIONS [a]

Sample No.	Trace No.[b]	Filament No.	Central Filament	C%[c]	MgB_2%[d]	dia., mm	H.T., C/min
A1	2555	36	Cu	2	25.0	0.92	700/60
A2	2510	36	Cu	2.5	22.6	0.92	675/60
A3	2580	36	Cu	3	17.8	0.91	650/120
A4	2538	36	Cu	3.5	25.8	0.91	675/60
A5	2535	36	Cu	4	26.9	0.91	675/60
C1	2584	36	Cu10Ni	2	23.3	0.92	700/60
C2	2760	36	Cu	2	26.9	0.92	675/60
C3	2687	30	Cu	2	14.2	0.83	675/60
C4	2814	30	Cu	2	17.7	0.83	675/60
C5	2823	24	Cu	2	11.9	0.92	650/120
C6	2627	24	Cu	2	14.2	0.83	675/60
C7	2774	18	Cu10Ni	2	20.5	0.83	675/60
C8	2590	18	Cu	2	22.0	0.83	675/60
C9	2748	6	Cu10Ni	2	26.0	0.83	675/60
C10	2575	1	-	2	17.6	0.83	675/60
D1	1990	1	-	1	11.5	0.83	675/20
D2	2823	24	Cu	2	11.9	0.96	675/60

[a]All strands use Nb barriers and Monel outer sheathes, with Mg:B atomic ratio = 1:2.

[b]Trace No.: sample number for internal purpose.

[c]C%: C doping level, which is based on C analysis by the LECO Corporation and normalized to the molar weight of MgB_2. No assumptions are made here concerning the expected uptake of C into the B sublattice.

[d]MgB_2%: cross sectional area fraction of MgB_2 in the whole strand.

TABLE II
VOLTAGE TAP POSITIONS ON STRANDS IN TRANSPORT VOLTAGE-CURRENT MEASUREMENTS (UNIT: MM)

Sample No.	D1			D2		
Voltage Tap No.	Left Contact[a]	Right Contact	Gauge Length[b]	Left Contact	Right Contact	Gauge Length
VT1	2.6	3.7	34.6	1.0	1.0	39.5
VT2	4.8	7.0	28.6	2.4	2.2	36.9
VT3	7.3	9.8	23.1	4.2	3.6	33.7
VT4	9.6	12.9	17.4	6.0	5.3	30.6
VT5	12.1	15.2	12.2	7.6	7.0	26.9
VT6	16.0	18.9	4.6	10.0	9.5	22.0
VT7				11.9	11.8	17.7
VT8				14.2	14.1	13.1
VT9				18.6	18.7	4.5

[a]Left contact is the separation between the left current contact and the left voltage tap; similarly right contact is the separation between the right current contact and the right voltage tap .

[b]Gauge length is the distance between the two contacts of a pair of voltage taps.

magnetic fields ranging from 0 T to 12 T. The transport J_c was determined following the electric field criterion E_c =1 μV/cm. Two kinds of samples were studied in this work: (1) "ITER Barrel" samples made with 1.5 m-long segments of A- and C-series strands helically wound onto 32-mm-diameter Ti-Al-V alloy holders [19]. The gauge length was 500 mm. (2) Short straight samples about 50 mm long were made from D- series strands. For these latter samples, either 6 or 9 pairs of voltage taps were attached onto the sample surface along the direction of the wire to detect the potential difference at different locations. After the measurements, all the voltages were translated into the electric fields, E, using voltage data divided by the gauge length of the specific voltage taps. For example, for sample D1, a series of voltage data $V(I)$ were obtained by the voltage tap VT8 at 7 T, then $E(I) = V(I)/(1.31\ \text{cm})$. Table II shows the exact positions of the voltage taps and the gauge lengths for each measurement.

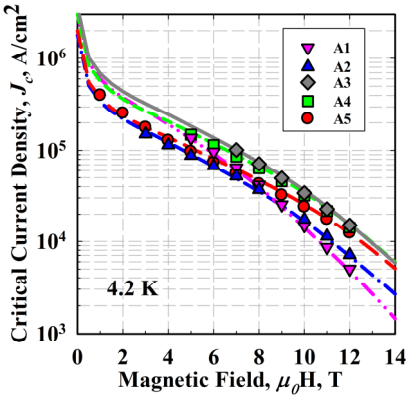

FIG. 1 Field dependence of the critical current density for A-series strands with different C concentration (lines are calculated by the percolation model)

TABLE III
FITTING PARAMETERS FOR THE PERCOLATION MODEL

Sample No.	J_{c0}, MA/cm^2	B_{c2}, T	γ	p_c
A1	3.0	25.2	2.6	0.25
A2	1.8	27.1	2.3	0.25
A3	3.6	27.1	2.2	0.25
A4	3.0	27.5	2.1	0.25
A5	2.0	27.9	2.05	0.25

The cross-sectional back scattered SEM images of D-series wires were pictured by Quanta 200 SEM.

III. RESULTS AND DISCUSSIONS

A. Critical Current Density of MgB_2 Long Strands

The A-series samples used boron powders with different carbon doping level ranging from 2-4 %. Since all the other processing parameters were kept constant including Mg:B atomic ratio, wire diameters, filament numbers and sheath and central-filament materials, it was reasonable to assume that the C content made major contributions to the change in J_c. Fig. 1 shows their critical current densities as a function of magnetic field. The best J_c was found to be 1.0×10^5 A/cm^2 at 4.2 K and 7 T, and was obtained for sample A3, which had 3% C doped boron powder. The field dependence of the transport J_c of series A samples were then fitted to the percolation model [20], with the resulting fitting curves shown in Fig. 1. The percolation model is based on the upper critical field anisotropy and the grain boundary pinning mechanism of MgB_2, combined with the percolation theory. Four parameters – the maximum pinning strength J_{c0}, the upper critical field B_{c2} and the anisotropy ratio γ are taken into account in fitting the J_c-$\mu_0 H$ performance. The forth parameter, the percolation threshold p_c, is fixed to 0.25 for simplicity. Table III lists the fitting parameters of each J_c-$\mu_0 H$ curve. As C doping level increases, B_{c2} (as extracted from the fit) increases from 25.2 T to 27.9 T, and γ drops from 2.6 to 2.05. These trends, in accord with previous reports [21], [22], may be due to the C substitution and possibly carbide nanoinclusions which exacerbate electron scattering and disorder in polycrystalline

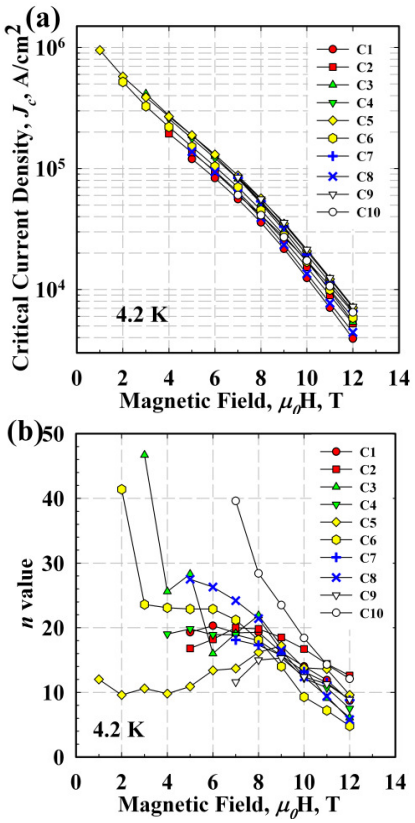

FIG. 2 Field dependence of (a) the critical current density and (b) *n*-values for C-series strands with different filament numbers at 4.2 K

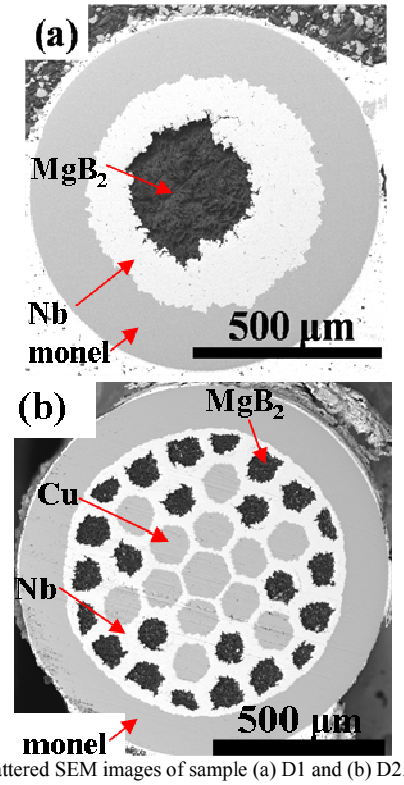

FIG. 3 Back scattered SEM images of sample (a) D1 and (b) D2.

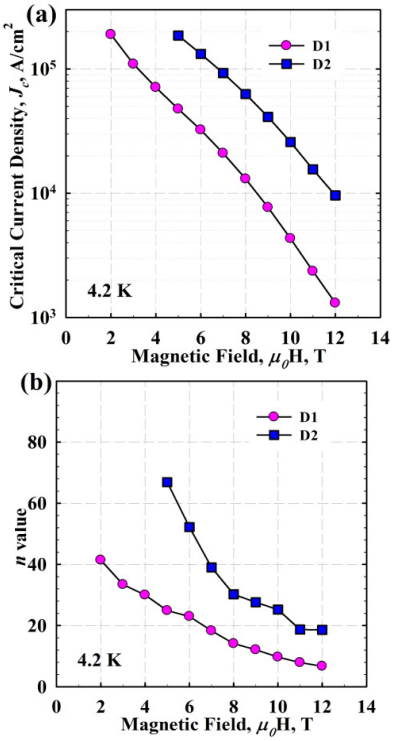

FIG. 4 The D-series Nb/Monel sheathed MgB_2 wires D1 (pink) and D2 (blue) in the current transfer length test showing good field dependence of (a) the critical current density and (b) *n*-values.

MgB_2. Also J_{c0}, representative of the pinning strength [23], reaches the maximum value of 3.6×10^6 A/cm^2 for sample A3 and then gradually decreases as additional carbon is introduced. It is widely accepted that proper C doping is helpful for the flux pinning [24]. However, given that too much C may deteriorate the connectivity and hence reduce the pinning strength, relatively low J_{c0}s are obtained for samples A4 and A5 after the best J_{c0} is achieved for sample A3.

A group of 2% C doped strands with different filament numbers is studied. As shown in Fig. 2(a), no obvious effect of filament numbers was observed with regard to J_c. As displayed in Fig. 2(b), *n*-values become somewhat diminished as a higher number of MgB_2 filaments are used in a strand. The single filament sample C10 shows the best *n*-values, nearly 40 at 7 T. However, *n*-values of some 30- or 36-filament strands, like C2 and C3, saturate at 20 when the applied field is lower than 8 T. The degradation of *n*-values for these multifilamentary wires is possibly caused by defects within the strands, such as filament sausaging, impurities, or voids and micro-cracks [25].

A. Current Transfer Length of MgB_2 Short Wires

Two Nb/Monel sheathed MgB_2 short wires, one monocore, the other a 24 count multifilamentary strand, were chosen to determine current transfer lengths, CTLs. The strand geometries of these wires are displayed in Fig 3. The MgB_2 filaments are embedded in a Nb chemical barrier and Monel outer sheath. For sample D2, there are 13 extra Cu filaments in the center of the wire for the purpose of drawability. The J_c-$\mu_0 H$ and *n*-value-$\mu_0 H$ relationships are presented in Figure 4, showing that they are high-performing strands.

Fig. 5 gives the electric field as a function of applied current

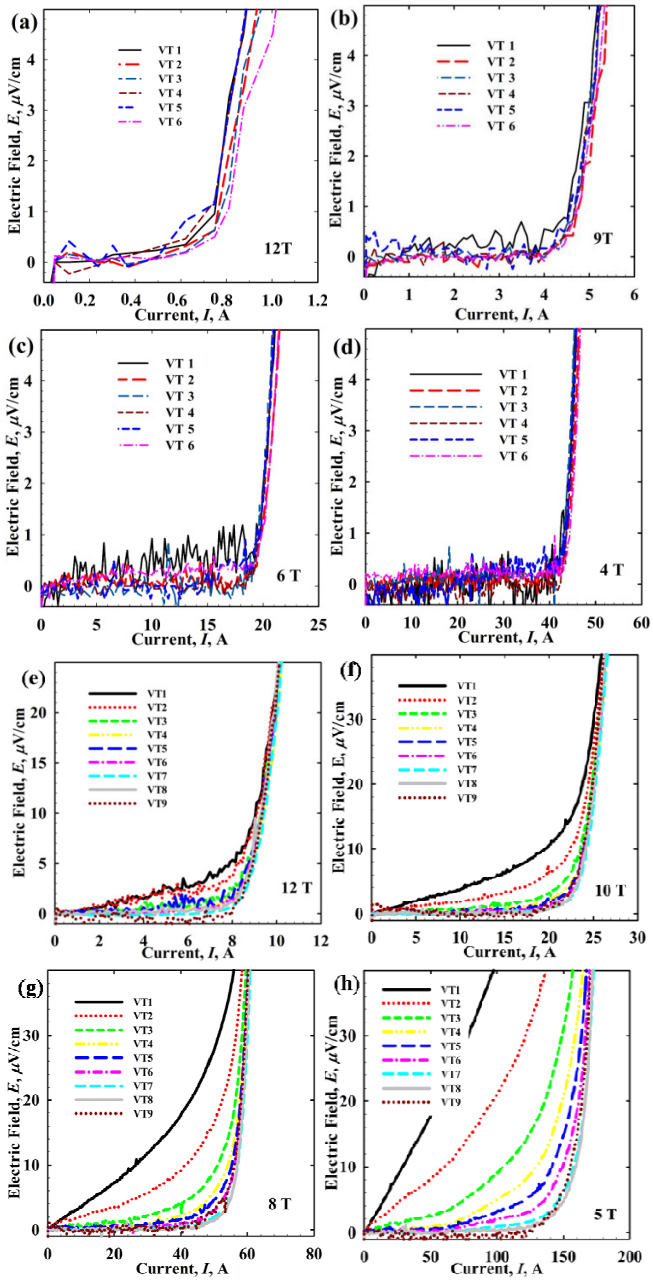

FIG. 5 *E-I* curves measured by different voltage taps at (a) 12 T, (b) 9 T, (c) 6 T, (d) 4 T for sample D1 and (e) 12 T, (f) 10 T, (g) 8 T, (h) 5 T for sample D2.

measured by variable voltage taps at certain magnetic fields. As shown in Fig 5(a)-(d), six *E-I* curves overlapped with each other from 4 to 12 T under the current of up to 40 A. This indicates that the CTL of the monocore wire D1 is less than the shortest measured distance between the current contact and the voltage tap contact, which is 3.7 mm. Compared with D1, sample D2 has a longer CTL; it is also field dependent. At 12 T, *E-I* curves measured by voltage taps VT1 and VT2 deviate from other curves in Fig. (e), indicating CTL is 2.2-3.6 mm. At 5 T, CTL increases to 9.5-11.8 mm. The difference of the CTL between D1 and D2 is due to the structural difference of the monocore and multifilamentary strands. D1 is a strand with the simplest wire geometry so the current can easily penetrate into the MgB_2 filament. Its CTL is so low that it cannot be accurately determined within the detection limit, let alone the field relationship of CTL. The slightly thicker wire D2 has a more complicated structure, with 24 MgB_2 filaments aligning in two circles, surrounding the central Cu filaments. To be homogeneously dispersed in the MgB_2 filaments, the current has to pass from the resistive outer sheath, through the Nb barrier, outer MgB_2 filaments and even possibly some Cu filaments, finally reaching the inner MgB_2 filaments. This process requires a somewhat larger CTL.

IV. Conclusion

The in-field critical current densities of a set of *in situ CTFF*-type *PIT* MgB_2 strands have been investigated in terms of C doping level, wire diameter and filament number. The strand with optimal doping level – 3% C achieved the best J_c of 1.0×10^5 A/cm^2 at 4.2 K, 7 T. By fitting it with the percolation model, the parameters showed that the B_{c2} and the flux pinning strength was improved and the anisotropy ratio was reduced. Increases in filament count did not change J_c, although *n*-values were higher for the monocore strand.

The current transfer length of MgB_2 strands with Nb chemical barriers and Monel sheaths increased with filament count. The CTL was less than 3.7 mm for the monocore strand, and it ranged from 2.2-11.8 mm for the 24- filamentary strand D2, depending on the applied field.

References

[1] J. Nagamatsu, N. Nakagawa, T. Muranaka, Y Zenitani and J. Akimitsu, "Superconductivity at 39 K in magnesium diboride," *Nature*, vol. 410, pp. 63-65, 2001

[2] S. X. Dou, O. Shcherbakova, W. K. Yeoh, J. H. Kim, S. Soltanian, X. L. Wang, C. Senatore, R. Flukiger, M. Dhalle, O. Hushjak and E. Babic, "Mechanism of enhancement in electromagnetic properties of MgB_2 by nano SiC doping," *Phys. Rev. Lett.,* vol. 98, p. 097002, 2007, 4pp.

[3] G. Z. Li, Y. Yang, M. A. Susner, M. D. Sumption and E. W. Collings, "Critical current densities and *n*-values of MgB_2 strands over a wide range of temperatures and fields," *Supercond. Sci. Technol.,* vol. 25, p. 025001, 2012, 10pp

[4] D. Wang, C. Wang, X. Zhang, Z. Gao, C. Yao, Y. Ma, M. Kanazawa, Y. Yamada, H. Oguro, S. Awaji and K. Watanabe, "Enhancement of J_c-B properties for binary and carbon-doped MgB_2 tapes by hot pressing," *Supercond. Sci. Technol.,* vol. 25, p. 065013, 2012, 5pp

[5] R. Flukiger, M. S. A. Hossain and C. Senatore, "Strong enhancement of J_c and B_{irr} in binary *in situ* MgB_2 wires after cold high pressure densification," *Supercond. Sci. Technol.,* vol. 22, p. 085002, 2012, 8pp

[6] W. Haessler, M. Herrmann, C. Rodig, M. Schubert, K. Nenkov and B. Holzapfel, "Further increase of the critical current density of MgB_2 tapes with nanocarbon doped mechanically alloyed precursor," *Supercond. Sci. Technol.,* vol. 21, p. 062001, 2008, 3pp .

[7] G. Giunchi, G. Ripamonti, E. Perini, T. Cavallin and E. Bassani, "Advancements in the reactive liquid Mg infiltration technique to produce long superconducting MgB_2 tubular wires," *IEEE Trans. Appl. Supercond.,* vol. 17, no. 2, pp. 2671-2676, 2007.

[8] H. Kumakura, J. Hur, K. Togano, A. Matsumoto, H. Wada and K. Kimura, "Superconducting properties of diffusion-processed multifilamentary MgB_2 wires," *IEEE Trans. Appl. Supercond.,* vol. 21, no. 3, pp. 2643-2649, 2011

[9] G. Z. Li, M. D. Sumption, M. A. Susner, Y. Yang, K. M. Reddy, M. A. Rindfleisch, M. J. Tomsic, C. J. Thong and E. W. Collings, "The critical current density of advanced internal-Mg-diffusion-processed MgB_2 wires," *Supercond. Sci. Technol.,* vol. 25, p. 115023, 2012, 8pp

[10] K. Adamczyk, A. Morawski, T. Cetner, A. Zaleski, D. Gajda, M. Rindfleisch, M. Tomsic, R. Diduszko and A. Presz, "Superconducting properties comparison of SiC doped multifilamentary MgB_2 wires of

various sheaths (Cu, Monel, Glidcop) after high pressure HIP treatment," *IEEE Trans. Appl. Supercond.*, vol. 22, no. 3, p. 6200204, 2012, 4pp

[11] K. Vinod, R. G. Abhilash Kumar and U. Syamaprasad, "Prospects for MgB_2 superconductors for magnet application," *Supercond. Sci. Technol.,* vol. 20, pp. R1-R13, 2007

[12] Y. Yang, M. A. Susner, M. D. Sumption, M. Rindfleisch, M. Tomsic and E. W. Collings, "Influence of strand design, boron type, and carbon doping method on the transport properties of powder-in-tube $MgB_{2-x}C_x$ strands," *IEEE Trans. Appl. Supercond.,* vol. 22, no. 2, p. 6200110, 2012, 10pp

[13] J. W. Ekin, "Current transfer in multifilamentary superconductors. I. Theory," *J. Appl. Phys.,* vol. 49, no. 6, pp. 3406-3409, 1978

[14] T. Holubek, P. Kovac and T. Melisek, "Current transfer length in MgB_2/Fe mono-core wire and approximation of the interface layer resistivity," *Supercond. Sci. Technol.,* vol. 18, pp. 1218-1221, 2005

[15] T. Holubek, M. Dhalle and P. Kovac, "Current transfer in MgB_2 wires with different sheath materials," *Supercond. Sci. Technol.,* vol. 20, pp. 123-128, 2007

[16] M. Wilson, Superconducting Magnets, 1st ed., Oxford: Clarendon, 1983, pp. 234-235

[17] M. Tomsic, M. Rindfleisch, J. Yue, K. McFadden, D. Doll, J. Phillips, M. D. Sumption, M. Bhatia, S. Bohnenstiehl and E. W. Collings, "Development of magnesium diboride (MgB_2) wires and magnets using in situ strand fabrication method," *Physica C,* vol. 456, pp. 203-208, 2007

[18] J. V. Marzik, R. C. Lewis, M. R. Nickles, D. K. Finnemore, J. Yue, M. Tomsic, M. Rindfleisch and M. D. Sumption, "Plasma synthesized boron nano-sized powder for MgB_2 wires," *AIP Conf. Proc.,* vol. 1219, pp. 295-302, 2010

[19] A. Hijhuis, W. A. J. Wessel, H. G. Knoopers, Y. Ilyin, A. della Corte and H. H. J. ten Kate, "Compressive prestrain in Nb_3Sn strand by steel tube and effect on the critical current measured on standard ITER barrel," *IEEE Trans. Appl. Supercond.,* vol. 15, no. 2, pp. 3466-3469, 2005

[20] M. Eisterer, M. Zehetmayer, and H. W. Weber, "Current percolation and anisotropy in polycrystalline MgB_2," *Phys. Rev. Lett.,* vol. 90, p. 247002, 2007, 4pp.

[21] T. Masui, S. Lee and S. Tajima, "Carbon-substitution effect on the electronic properties of MgB_2 single crystals," *Phys. Rev. B,* vol. 70, p. 024504, 2004, 7pp.

[22] S. Oh, J. H. Kim, K. Cho, C Lee, C. Kim, S. X. Dou, M. Rindfleisch, M. Tomsic and J. Ahn, "A comparative study on field, temperature, and strain dependence of the critical current for doped and undoped MgB_2 wires based on the percolation model," *J. Appl. Phys.,* vol. 106, p. 063912, 2009, 5pp.

[23] M. Eisterer, C. Krutzler and H. W. Weber, "Influence of the upper critical-field anisotropy on the transport properties of polycrystalline MgB_2," *J. Appl. Phys.,* vol. 98, p. 033906, 2005, 5pp.

[24] S. X. Dou, S. Soltanian, W. K. Yeoh and Y. Zhang, "Effect of nano-particle doping on the upper critical field and flux pinning in MgB_2," *IEEE Trans. Appl. Supercond.*, vol. 15, no. 2, pp. 3219-3223, 2005

[25] V. Braccini, D. Nardelli, R. Penco and G. Grasso, "Development of *ex situ* processed MgB_2 wires and their applications to magnets," *Physica C*, vol. 456, pp. 209-217, 2007